Article

Comparative Study on Metabolic Regulation of SAP Deletion in Normal Mice and Atherosclerotic Mice

Yifan Zhu [1], Shuhan Xie [2,†], Hailong Shu [3,†], Yiqing Lu [4], Jiawei Guo [4], Qian Li [2], Yongli Zhang [2], and Yongxia Yang [3,*]

[1] Department of Thyroid Surgery, the First Affiliated Hospital of Sun Yat-sen University, Guangzhou 510080, China
[2] School of Basic Medicine, Guangdong Pharmaceutical University, Guangzhou 510006, China
[3] School of medical Information and Engineering, Guangdong Pharmaceutical University, Guangzhou 510006, China
[4] School of Life Sciences and Biopharmaceuticals, Guangdong Pharmaceutical University, Guangzhou 510006, China
* Correspondence: yangyongxia@gdpu.edu.cn, Tel.: +86-(0)20-3935-2197
† These authors contributed equally to this work.
Received: 25 December 2024; Revised: 13 January 2025; Accepted: 27 June 2025; Published: 11 July 2025

Abstract: SAP is a serum protein associated with an increased risk of cardiovascular events, and studies have uncovered a significant positive correlation between SAP and the pathogenesis of atherosclerosis. Our previous research found that SAP deficiency in ApoE$^{-/-}$ mice significantly reduced the formation of foam cells and the expression of pro-inflammatory factors, and caused significant metabolic changes. However, it is still unclear whether SAP deficiency has the same function and metabolic regulation effect on normal background mice. In this study, C57 and SAP$^{-/-}$ mice were used as models. Histopathological examinations were performed to evaluate the histomorphological changes of heart, liver, spleen, lung and kidney tissues in SAP$^{-/-}$ mice. The results showed that there were no significant histopathology changes in the main organs of SAP$^{-/-}$ mice, but there were significant differences in the serum metabolic profiles between C57 and SAP$^{-/-}$ mice. It was found that the deficiency of SAP in both C57 and ApoE$^{-/-}$ mice upregulated choline, but the regulatory trends on LDL/VLDL were different. Acetate and pyruvate were regulated by SAP deficiency in ApoE$^{-/-}$ mice, but not in C57 mice. In addition, the deletion of SAP also caused significant changes in formate, tyrosine, glycine, glucose, TMAO, taurine, citrate, succinate, and histidine in C57 context, which were not detected in the context of atherosclerosis. In summary, this study indicates that the metabolic regulation of the SAP gene is not only related to the gene itself but also related to the physiological or pathological state of the organism.

Keywords: ^{1}H-NMR; metabolomics; atherosclerotic; Serum amyloid P protein (SAP)

1. Introduction

Serum amyloid P protein (SAP) is a member of the pentapeptide protein family [1], and it involves many activities, such as innate immunity, inflammatory reaction, and amyloidosis in the body [2,3]. SAP is usually synthesized and secreted by liver cells with an approximate half-life of 24 h. Moreover, SAP can also be produced by macrophages and smooth muscle cells in some diseases, i.e., atherosclerosis [4]. Cox N et al. [5]. found that SAP directly binds to monocytes, neutrophils and macrophages, altering their activation and differentiation, thereby regulating immune response. In addition, it was reported that SAP can interact with pathogens and cell debris to activate the complement pathway and promote macrophages and neutrophils to clear the pathogens and cell debris [6].

In recent years, the role of SAP in cardiovascular disease has been gradually recognized. SAP is a serum protein associated with an increased risk of cardiovascular events [7,8]. It has been discovered that antagonizing SAP protein can improve systemic amyloidosis [9]. In the cardiovascular system, SAP is defined as one of the main causes of cardiac amyloidosis [10,11]. Li et al. [12]. found that SAP was significantly and positively correlated with the pathological process of atherosclerosis. Our previous research found that the absence of SAP can significantly reduce the formation of foam cells and the expression of pro-inflammatory factors in atherosclerosis [13]. We confirmed through metabonomics that deletion of the SAP gene regulated the metabolism of acetate, pyruvate, choline, and VLDL/LDL in ApoE$^{-/-}$ mice, and these metabolites were significantly correlated

with atherosclerosis [14]. However, does the deletion of SAP have the same functional and metabolic regulation effects on normal background mice? There is no recent report.

Metabonomics is the comprehensive characterization of small molecule metabolites in cells, tissues, organs and organisms that can respond to metabolic changes caused by intrinsic or extrinsic factors. In recent years, the field of metabonomics has undergone rapid development, enabling the study of metabolic diseases [15,16]. ^{1}H-NMR has become an effective technique for metabonomics research because it does not require special sample processing and is easy to operate. Based on ^{1}H-NMR, Loanna Tzoulaki et al. found that atherosclerosis was significantly correlated with lipid metabolism, fatty acids, carbohydrates, aromatic amino acids, and TCA cycle [17]. We demonstrated that the deletion of P-selectin glycoprotein ligand-1 (PSGL-1) gene can regulate glucose metabolism, lipid metabolism, amino acid and phospholipid metabolism in atherosclerosis at the metabolic level [18].

In this report, ^{1}H-NMR metabonomics was used to study the effect of the SAP gene deletion on the phenotype and metabolism of normal mice, and differences in the metabolic regulation of SAP on atherosclerosis mice and normal mice were compared to provide a basis for clarifying the function of SAP.

2. Materials and Methods

2.1. Laboratory Animals

Serum amyloid P component deficient mice ($SAP^{-/-}$, C57 background) were provided by the Institute of Biochemistry and Cell Biology. C57 mice were purchased from Guangdong Medical Laboratory Animal Center (GDMLAC). All mice were placed in an SPF environment. There were 10 mice in each group. GDMLAC provided both normal and high-fat diets (normal 87.5%, cholesterol 2%, bile salt 0.5%, lard 10%) consumed by animals. The normal diet was replaced with a high-fat diet at 8 weeks of age, and the diet was stopped at 16 weeks of age.

2.2. Histopathological Examinations

H&E staining was performed to evaluate the histomorphological changes in $SAP^{-/-}$ mice. Tissues of heart, liver, spleen, lung and kidney form C57 and $SAP^{-/-}$ mice were taken overnight and fixed with 4% formalin. The tissues are dehydrated, embedded in paraffin and cut into 4 μm fragments. Paraffin sections are hydrated, deparaffined and stained with hematoxylin and eosin.

2.3. Blood Collection

Blood was drawn from mice at 8 weeks, 8 + 4 weeks (normal diet for 8 weeks, high-fat diet for 4 weeks), and 8 + 8 weeks (normal diet for 8 weeks, high-fat diet for 8 weeks) through the orbital venous plexus for use. After the mice were routinely anesthetized, a 1 cm capillary tube was inserted under the eyeball of each mouse. About 600 μL of blood was collected from each mouse and left to sit for 2 h. The blood sample was then centrifuged at 5000 rpm for 30 min to obtain serum.

During sample collection, hemolysis or contamination was inevitable, which led to the samples not meeting the experimental conditions. We controlled the quality of all samples, and finally obtained 9 samples of 8-week C57 mice serum, 10 samples of 8 + 4-week C57 mice serum, and 9 samples of 8 + 8-week C57 mice serum, and about $SAP^{-/-}$ mice, we obtained 8 samples of 8-week mice serum, 8 samples of 8 + 4-week mice serum, and 7 samples of 8 + 8-week mice serum. Serum samples were stored in a −80 °C refrigerator.

2.4. ^{1}H-NMR Spectroscopy

The serum samples were thawed and centrifuged at 4 °C for 10 min (12,000 rpm). A total of 250 μL serum was added to a 5 mm NMR tube with 150 μL PBS (0.2 mol/L, pH 7.4) and 100 μL D2O. Bruker AVANCE III 500 MHz Superconducting NMR Spectrometer (Bruker, Inc., Billerica, MA, USA) was used to acquire serum ^{1}H-NMR spectra with Carr-Purcell-Meiboom-Gill[CMPG, recycle delay-90-(τ-180-τ)n- acquisition] pulse sequence. The probe temperature is 298 K. Total echo time is 100 ms (2 nτ). The relaxation delay time was set to 3 s. The spectrum width was 10 kHz and the collection times were 128. Topspin 4.0 software was used for manual phase adjustment and baseline correction. The chemical shift was calibrated with lactic acid bimodal δ1.33. AMIX (V4.0. Bruker Biospin, Karlsruhe, Germany) was used for integrating peaks at δ0.5–9.0. The integrals of δ4.7–5.5 were set to zero to eliminate the effect of residual water signal. 0.04 ppm was used as the integration interval to perform equal interval integration. The integral was normalized to the sum of spectral integrals, and the percentage of each peak area to the total peak area was calculated.

2.5. Bioinformatics Analysis of Metabolites by SAP

The protein-protein interaction (PPI) network of the SAP gene was constructed using the STRING database (version 12.0; https://string-db.org/, accessed on 12 October 2022). The canonical protein name SAP was queried in the Mus musculus (mouse) genome. The confidence score threshold was set to ≥0.7 (high confidence) to ensure high-confidence interactions. Utilizing the "ClusterProfiler" R package, Kyoto Encyclopedia of Genes and Genomes (KEGG) and Gene Ontology (GO) assessments were executed to pinpoint gene functions and cellular routes that were abundant in the network's core genes.

2.6. Statistical Methods

Two statistical methods, PCA and OPLS-DA, were used in our study. PCA is an unsupervised dimension reduction analysis method, which can reduce the dimensions of high-dimensional metabolome data to low dimensions and show the similarities or differences between samples in the low-dimensional space, so as to help us better understand the structure of metabolome data and the relationship between samples. OPLS-DA is a supervised multiple linear regression analysis method, that divides variables in metabolome data into classification prediction and correlation interpretation by establishing an optimal linear model. OPLS-DA can not only accurately distinguish samples from different taxa, but also find metabolites related to taxa.

In OPLS-DA, VIP values were used to measure the contribution of each metabolite to the model. The higher the VIP value, the more important this metabolite is to distinguish between different groups of samples.

To ensure the reliability of the OPLS-DA model, we conducted 200 replacement tests on the model. R2 is the fitting ability index of the model, which represents how much variance the model can explain in the data. The closer the value is to 1, the better the fitting ability of the model is. Q2 is an indicator of the model's predictive ability, indicating the model's predictive ability for unknown data. The closer the value is to 1, the better the prediction ability of the model is.

A heat map is a visual tool commonly used to show the relationships between variables and samples in metabonomics data. Heat maps indicate similarity or difference by arranging variables or samples on horizontal and vertical axes, respectively, and using color coding. By looking at the heat map, we can quickly spot patterns and trends in the data.

3. Result

3.1. Histopathological Evaluation

At 8 + 8 w, tissues of the heart, liver, spleen, lung and kidney in C57 and $SAP^{-/-}$ mice were collected for H&E staining (Figure 1). The pathological results showed no significant difference in the histomorphology of the five kinds of tissues between $SAP^{-/-}$ mice and C57 mice, indicating that the deletion of the SAP gene did not cause pathological changes in the main organs of C57 mice.

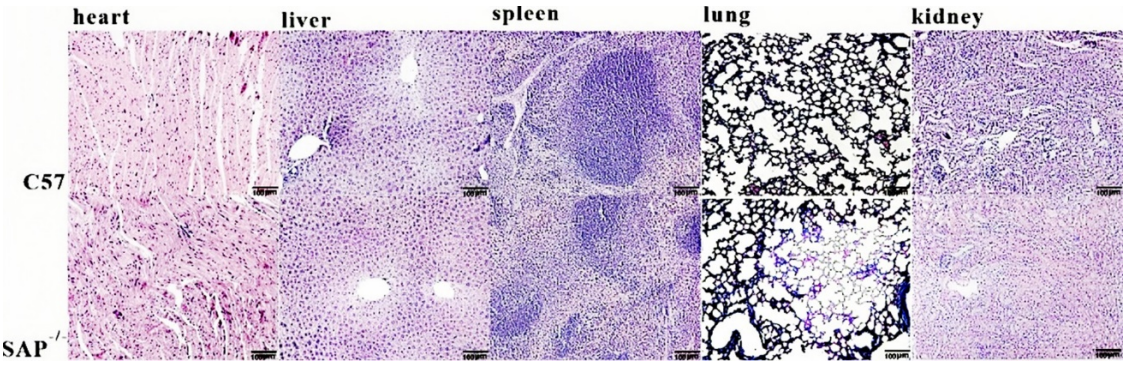

Figure 1. Hematoxylin-eosin staining of heart, liver, spleen, lung and kidney tissues in C57 mice and $SAP^{-/-}$ mice.

3.2. Metabolite Profilings of Serum Samples

Figure 2 shows the typical serum ^{1}H-NMR spectra of C57 (Figure 2A) and $SAP^{-/-}$ mice (Figure 2B). Based on previous studies [19–21], the biomagnetic resonance database (BMRB, https://bmrb.io/, accessed on 24 October 2022) and the Human metabolome database (HMDB, https://hmdb.ca/, accessed on 24 October 2022), 25 metabolites were identified. The spectra were recorded at a 100-fold amplification to enhance the clarity of the peaks.

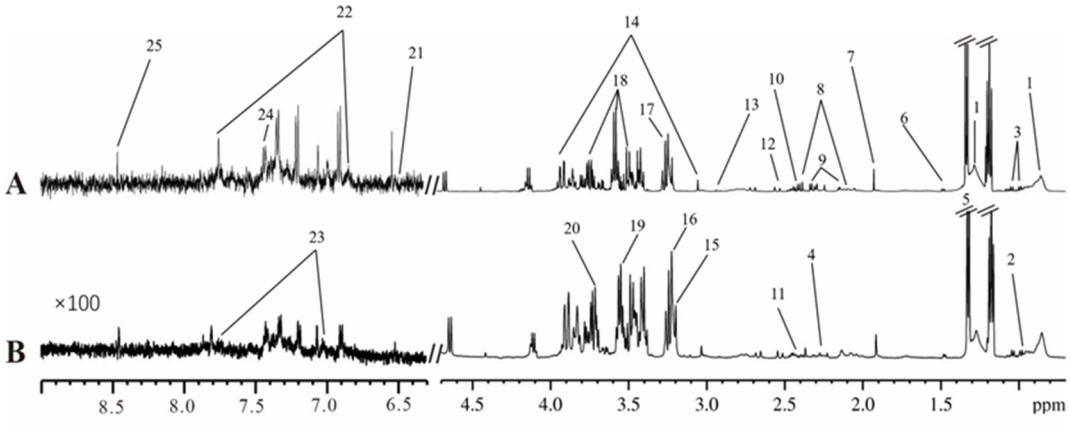

Figure 2. Representative serum ^{1}H NMR spectra of (**A**) C57 mice and（**B**）SAP$^{-/-}$ mice. 1. VLDL + LDL. 2. leucine/isoleucine. 3. valine. 4. α-ketoglutarate. 5. lactate. 6. alanine 7. acetate. 8. glutamine. 9. acetoacetate. 10. pyruvate. 11. succinate. 12. citrate. 13. dimethylamine. 14. creatine. 15. choline. 16. TMAO. 17. taurine. 18. α,β-glucose. 19. glycine. 20. glyceride. 21. fumarate. 22. tyrosine. 23. histidine. 24. phenylalanine. 25. formate.

3.3. Multivariate Statistical Analysis

After ^{1}H NMR normalization, principal component analysis (PCA) was performed on the serum spectra data of C57 and SAP$^{-/-}$ groups at different experimental stages. Unsupervised discriminant model PCA can observe the natural clustering trend between the two groups, and the results are shown in Figure 3. During the whole stages, there were significant differences between the two groups at 8 w, 8 + 4 w, and 8 + 8 w, indicating significant differences in serum metabolic profiles. It was found that the metabolic difference occurred at 8 w and these differences remained until 8 + 8 w, which revealed the metabolic changes in SAP$^{-/-}$ mice were not correlated with a high-fat diet. The results showed that The SAP gene deletion caused significant metabolic changes under the C57 background.

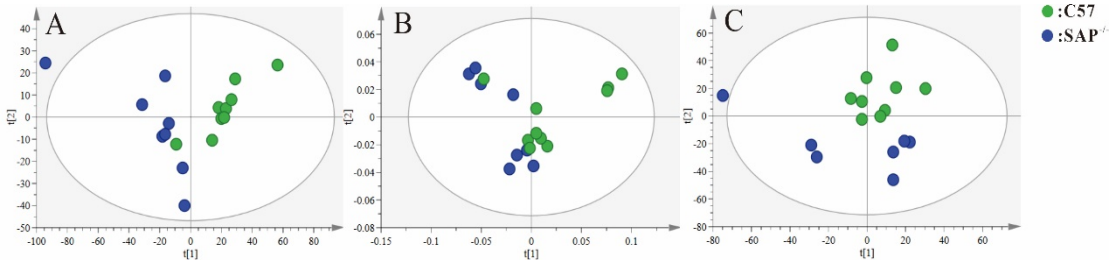

Figure 3. PCA scores plots for serum ^{1}H NMR spectra data. (**A**) 8 w, R2X = 0.775, Q2 = 0.548; (**B**) 8 + 4 w, R2X = 0.785, Q2 = 0.625; (**C**) 8 + 8 w, R2X = 0.981, Q2 = 0.793.

Orthogonal Partial minimum discriminant analysis (OPLS-DA) is a supervised discriminant analysis method used to identify the differential metabolites. OPLS-DA was performed on the two groups at different periods and the corresponding VIP values were obtained (Figure 4). 200 replacement tests were conducted on all OPLS-DA models (Figure A1). The metabolites with VIP > 1 were then statistically analyzed by GraphPad prism8.0.1 (*t* test). The differential metabolites were identified based on p ($p < 0.05$) and VIP (VIP > 1) values (Table 1). Based on data in Table 1, we concluded that the metabolites of formate, TMAO, tyrosine, citrate, VLDL + LDL, succinate, α- ketoglutarate, valine, glycine, histidine, glucose, taurine and choline were significantly altered following SAP deletion in the C57 background.

Cluster analysis was performed and a heat map of all metabolites was plotted at the three period (Figure. 5A–C), in which the change trend of all metabolites between the two groups could be clearly observed. It was found that all SAP$^{-/-}$ serum samples were well clustered together and they were clearly differentiated from C57 mice, which is consistent with the findings in PCA. The results showed that SAP$^{-/-}$ mice and C57 mice had significantly different metabolic characteristics.

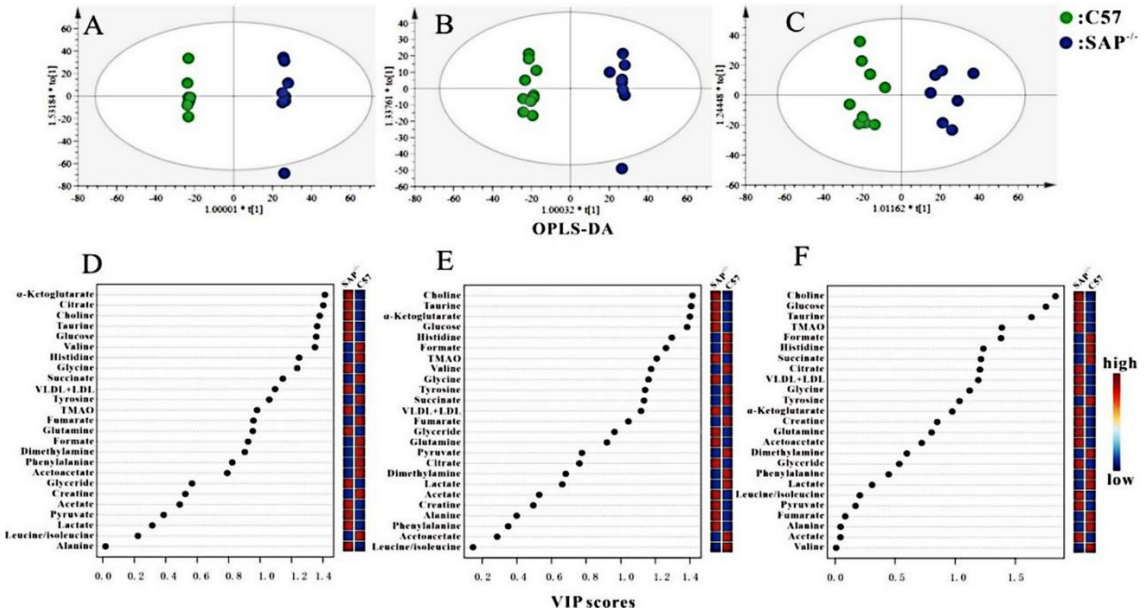

Figure 4. Metabolic differences between C57 and SAP$^{-/-}$ groups at three periods. OPLS-DA scores plots (**A**) (8 w), (**B**) (8 + 4 w), (**C**) (8 + 8 w) and the corresponding VIP values (**D**) (8 w), (**E**) (8 + 4 w), (**F**) (8 + 8 w).

Table 1. Statistical analysis of potential biochemical markers in serum of SAP$^{-/-}$ mice.

Metabolite	δ^1H (ppm)	Pathway	8 w	8 + 4 w	8 + 8 w
Formate	8.46	Ketone metabolism	-	↓***	↓**
Tyrosine	6.89 7.81	Amino acid metabolism	↓**	↓***	↓*
Glycine	3.55	Amino acid metabolism	↑***	↑***	↑*
Glucose	3.45 3.75 3.82	Glucose metabolism	↑***	↑***	↑***
TMAO	3.26	TMA-TMAO	-	↑***	↑**
Taurine	3.25	Amino acid metabolism	↑***	↑***	↑***
Choline	3.2	Lipid metabolism	↑***	↑***	↑***
Citrate	2.54	Energy metabolism	↑***	-	↑*
Succinate	2.41	Energy metabolism	↓***	↓***	↓*
α-Ketoglutarate	2.28	Glucose metabolism	↑***	↑***	-
Valine	0.97 1.02 2.24	Amino acid metabolism	↓***	↓***	-
VLDL + LDL	0.88 1.28	Lipid metabolism	↑**	↑**	↑*
Histidine	7.04 7.74	Amino acid metabolism	↓***	↓***	↓**

Note: compared with C57, ↑ denotes the increase, - denotes no statistical change and ↓ denotes the decrease in SAP$^{-/-}$ mice; * $p < 0.05$, ** $p < 0.01$, *** $p < 0.001$.

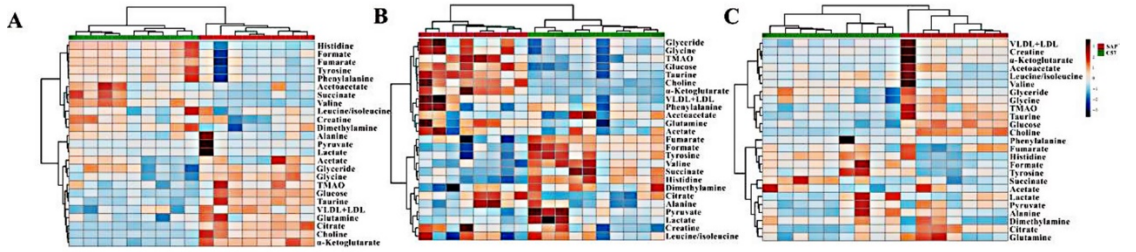

Figure 5. Heat maps of metabolites in C57 and SAP$^{-/-}$ mice. (**A**) (8 w), (**B**) (8 + 4 w), (**C**) (8 + 8 w).

3.4. Results of Bioinformatics Analyses of Metabolites by SAP

Figure 6A shows the SAP protein-protein interaction (PPI) network, which is found to consist of 11nodes: Mbl1, Hrg, Fn1, Fcgr2b, Crp, Ttr, Afm, Alb, Pzp, Masp2 and SAP. GO and KEGG enrichment analyses were performed on the genes identified in the PPI network (Figure 6B,C). The enriched metabolic pathways mainly included thyroid hormone synthesis, complement and coagulation cascade. This result suggested that SAP may influence metabolic processes through these pathways. To verify the influence of SAP on metabolites, we analyzed

the correlation between some key genes of the metabolites screened above and SAP. Figure 6D showed that SAP was negatively correlated with SLC6A6, FMO3, GCH1 and ACLY, while positively correlated with PAH gene. SLC6A6 was found to be responsible for the intracellular and extracellular transport of taurine. FMO3 oxidizes TMA to TMAO. ACLY catalyzes the conversion of citric acid to acetyl-CoA and is associated with lipid metabolism. Therefore, low expression of SAP can lead to increased taurine, TAMO, citrate, and VLDL + LDL. The PAH gene encodes phenylalanine hydroxylase (PAH), a rate-limiting enzyme that converts phenylalanine to tyrosine. Low expression of SAP can lead to decreased tyrosine. The results of these bioinformatics studies were consistent with ours. Other metabolic changes may be caused by synergies between SAP and its associated genes. However, it is important to note that the results of bioinformatics analysis may be related to the selected database and the source of the database. So, in the future, we will conduct molecular biology experiments on cells to verify all the key genes associated with differential metabolites.

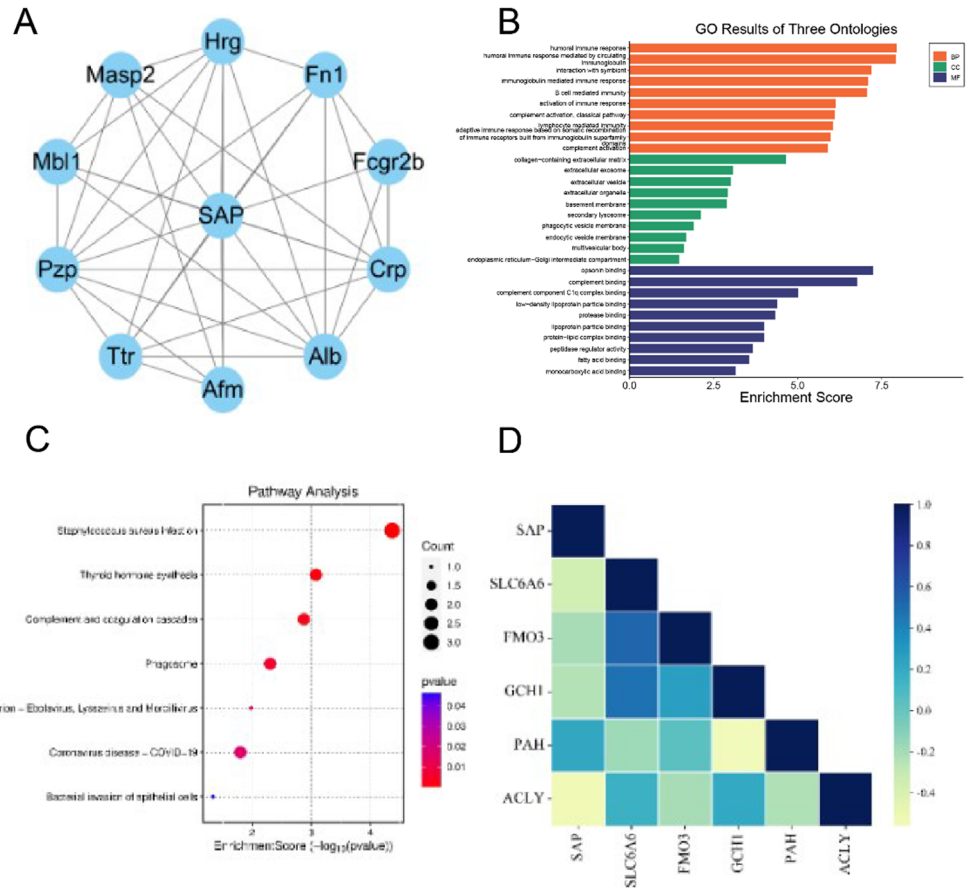

Figure 6. Analysis of the role of SAP genes. (**A**) Protein-Protein Interaction Network of SAP. (**B**) GO enrichment analyses were performed on the genes of the PPI network. (**C**) KEGG enrichment analyses were performed on the genes of the PPI network. (**D**) Correlation analysis of SAP with key metabolite genes.

4. Discussion

Atherosclerosis is characterized by impaired glucose and lipid metabolism. Li et al. confirmed the existence of co-localization of SAP protein and atherosclerotic lesions [12]. Here, the results indicated that deletion of the SAP gene inhibited the progression of atherosclerosis [13], and the levels of pyruvate, acetate, choline and VLDL + LDL were altered throughout the progression of AS [14]. In this study, we compared the differences in metabolic regulation induced by the SAP gene deletion on C57 background ($SAP^{-/-}$ mice) and the spontaneous atherosclerosis model of $ApoE^{-/-}$ mice ($ApoE^{-/-}$; $SAP^{-/-}$ mice) (Table 2).

Although no histological changes in the main organs in $SAP^{-/-}$ mice were found, significant metabolic changes have already occurred. It was found that the absence of SAP in both C57 and $ApoE^{-/-}$ mice can cause an upregulation of choline. However, these two models have different regulatory trends towards LDL/VLDL. Acetate and pyruvate were regulated by SAP deficiency in$ApoE^{-/-}$ mice, but not regulated in C57 environment. In addition, the deletion of SAP also caused significant changes in formate, tyrosine, glycine, glucose, TMAO, taurine, citrate, succinate, and histidine in C57 context, which were not found in $ApoE^{-/-}$ mice. Therefore, the regulatory effect of

SAP deficiency on metabolism is not only related to the gene itself, but also to the physiological and pathological state of the organism. In normal background mice and atherosclerosis mice models, the metabolic changes caused by SAP deletion are significantly different.

Table 2. Statistical analysis of potential biochemical markers in $ApoE^{-/-}$, $ApoE^{-/-}$;$SAP^{-/-}$ and $SAP^{-/-}$ mice at 8 + 8 w.

Metabolites	δ1 H (ppm)	Pathway	$ApoE^{-/-}$ VS. C57	$ApoE^{-/-}$; $SAP^{-/-}$ VS. $ApoE^{-/-}$	$SAP^{-/-}$ VS. C57
Formate	8.46	Ketone metabolism	↓**	-	↓**
Tyrosine	6.89 7.81	Amino acid metabolism	↓***	-	↓*
Fumarate	6.51	Energy metabolism	↓***	-	-
Glycine	3.55	Amino acid metabolism	-	-	↑*
Glucose	3.453.75 3.82	Glucose metabolism	-	-	↑***
TMAO	3.26	TMA-TMAO	-	-	↑**
Taurine	3.25	Amino acid metabolism	-	-	↑***
Choline	3.2	Lipid metabolism	↓**	↑**	↑***
Citrate	2.54	Energy metabolism	-	-	↑*
Succinate	2.41	Energy metabolism	-	-	↓*
Pyruvate	2.37	Energy metabolism	↑**	↓***	-
Acetoacetate	2.28	Energy metabolism	↓**	-	-
Acetate	1.92	Ketone metabolism	↓*	↑*	-
VLDL + LDL	0.88 1.28	Lipid metabolism	↑**	↓**	↑*
Histidine	7.04 7.74	Amino acid metabolism	↓***	-	↓**

Note: ↑, the increase; ↓, the decrease; compared with C57 mice, * $p < 0.05$, ** $p < 0.01$, *** $p < 0.001$, -, no statistical change.

Choline has positive emulsifying properties, which can prevent cholesterol from depositing on the inner wall of blood vessels and remove some deposits, thereby improving the absorption and utilization of fat [22,23]. It was found that the deletion of The SAP gene increased the level of choline in the serum of normal and atherosclerotic mice, which indicated that the regulation of choline by The SAP gene was independent of the disease status. Also, the levels of VLDL and LDL in the serum of $SAP^{-/-}$mice increased compared to C57 mice. However, VLDL and LDL in $ApoE^{-/-}$; $SAP^{-/-}$ mice were reduced. The pathological process of atherosclerosis is closely related to the severity of plasma hyperlipidemia. In clinical practice, the plasma concentration of VLDL and LDL is used as one of the diagnostic criteria for hypercholesterolemia [21]. SAP has a high affinity for serum lipoprotein and deposits on the walls of blood vessels in the form of amyloid [4,24]. We speculated that the regulation of VLDL + LDL by The SAP gene deletion was related to the pathological state of the organism. Under normal physiological conditions, deletion of the SAP gene can prevent more VLDL + LDL deposition, while in atherosclerotic pathological conditions, deletion of the SAP gene can promote the clearance of more VLDL + LDL. In addition, we found that the levels of acetate and pyruvate in $ApoE^{-/-}$; $SAP^{-/-}$ mice were restored to normal levels in C57 mice, but these two metabolites were not altered in $SAP^{-/-}$ mice. Through comparative analysis, we found that the regulation of choline caused by SAP deletion is actually caused by the gene itself, which has nothing to do with the physiological or pathological state of the organism. However, the regulation of acetate, pyruvate, VLDL and LDL by SAP deficiency is related to the state of the organism, and is the result of the combination of gene and disease state.

The study showed that SAP deficiency on C57 background ($SAP^{-/-}$ mice) did not cause morphological changes in major organs, but significant changes in serum metabolic profiles. The metabolic changes of $SAP^{-/-}$ mice were summarized in Figure 7. It was found that citrate and α-ketoglutarate, two important intermediates of TCA cycle, were significantly increased in $SAP^{-/-}$ mice. Glucose, the initiator of energy metabolism, was significantly decreased, suggesting that the deletion of $SAP^{-/-}$ gene induced the imbalance of energy metabolism. Notably, the levels of nonessential amino acid tyrosine and essential amino acid valine in $SAP^{-/-}$ mice show a downward trend. Tyrosine, as a raw material for synthesizing catecholamines in vivo, regulates the neural activity of mice to a certain extent [25]. Valine is absorbed by nerve cells as a raw material for energy metabolism. It plays a major role in the transamination of amino acids, nitrogen metabolism and the body's neural activities [26]. The changes in these two metabolites may indicate that the deficiency of the SAP gene has a certain impact on the neural activity of mice.

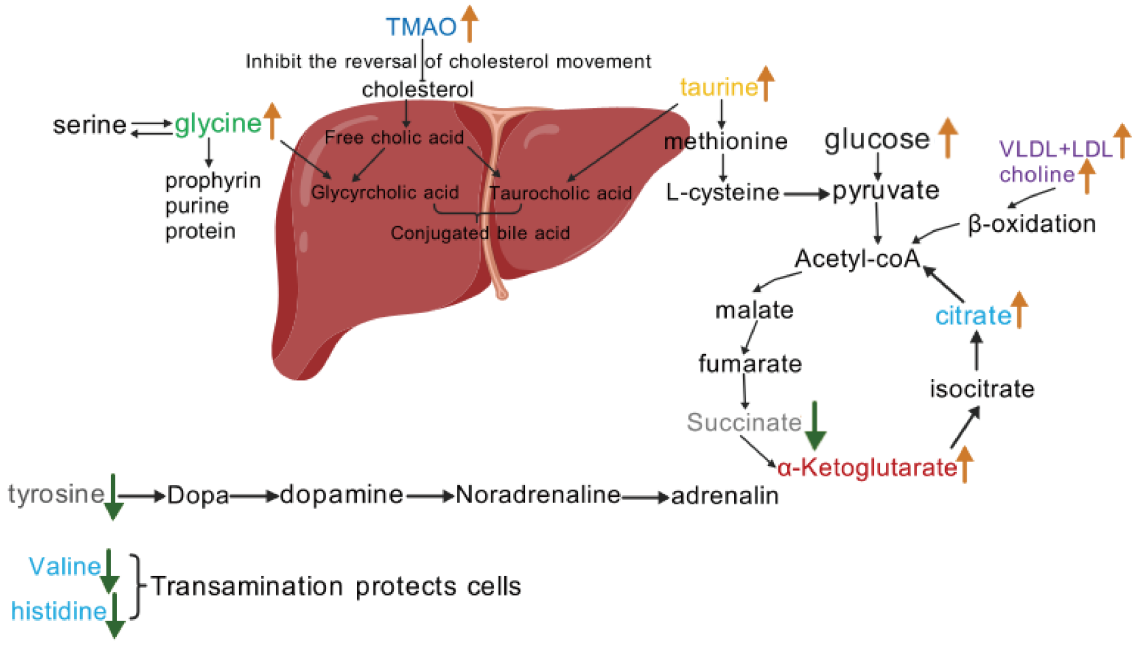

Figure 7. Pathway map of metabolic changes in SAP$^{-/-}$ mice compared with C57 mice. ↓: decrease in serum, ↑: increase in serum.

Histidine can cross the blood-brain barrier and be converted into histamine through histidine decarboxylase [27], mediating inflammation and allergic reactions. In addition, histidine is an inhibitor of mitochondrial glutamine transporters, which can protect cells from ammonia toxicity [28]. Glycine, as one of the main amino acids that provide a carbon unit, maintains cell stability by integrating cell states through the input of carbon units in cellular carbon metabolism [24]. Glycine is also involved in the synthesis of bile acids and promoting the conversion of cholesterol in the body [29]. The decrease of glycine and histidine in SAP$^{-/-}$ mice indicated that the deletion of the SAP gene might reduce the stability of somatic cells.

Taurine is a cysteine derivative synthesized by pancreas, and stored in various tissues and cells [30]. It plays an important role in various physiological processes, including bile acid synthesis, cell membrane stability, calcium flow regulation, and immune regulation [31]. In this study, pancreatic tissue showed no pathological changes, but serum taurine in SAP$^{-/-}$ mice significantly increased, indicating that metabolic abnormalities had already occurred before significant changes in tissue morphology. TMA, produced by the metabolism of lecithin and choline, is oxidized to TMAO by intestinal flora [32]. The study found elevated serum TMAO in SAP$^{-/-}$ mice. It was speculated that this was due to the increase of choline in SAP$^{-/-}$ mice, and thus increased the expression of TMA. As the raw material for TMAO production, TMA directly determines the level of serum TMAO. However, whether the deficiency of the SAP gene changes the intestinal environment or gut flora of mice needs more studies. In conclusion, it was showed that formate, tyrosine, glycine, glucose, TMAO, taurine, choline, citrate, succinate, α-ketoglutarate, valine, VLDL + LDL and histidine were regulated in SAP$^{-/-}$ mice during the whole experimental periods.

5. Conclusions

Based on ^{1}H NMR metabonomics and multivariate data analysis, the study shows that although the SAP deficiency does not alter the tissue structure of main organs, significant metabolic changes were observed in SAP$^{-/-}$ mice. It was found that SAP deficiency has a regulatory effect on energy metabolism, neural activity, cell stability, and immune regulation. As intermediates and final products of biochemical pathways, metabolites are not only regulated by genes, but also influenced by the physiological or pathological state of the organism. The overall metabolic phenotype is the result of a combination of multiple factors. We found that the same gene has different metabolic regulatory effects on physiological or pathological states. In this study, based on ^{1}H NMR metabonomics, the metabolic regulation of the SAP gene deletion in normal and atherosclerotic background was compared to reveal the function of the SAP gene.

Author Contributions: Y.Z. (Yifan Zhu): Conceptualization, Methodology, Validation, Formal analysis, Investigation, Writing—original draft, Visualization; S.X. and H.S.: Conceptualization, Methodology, Validation, Formal analysis, Investigation, Visualization; Y.L.: Conceptualization, Methodology, Formal analysis, Investigation, Editing; J.G.: Methodology, Validation, Formal analysis, Visualization; Q.L.: Methodology, Investigation, Visualization; Y.Z. (Yongli Zhang): Conceptualization,

Supervision, Project administration; Y.Y.: Conceptualization, Supervision, Project administration, Writing—Reviewing & Editing, Funding acquisition. All authors have read and agreed to the published version of the manuscript.

Funding: This work was supported by the National Natural Science Foundation of China (No.22074024, 21005022), Key scientific research platforms and projects of Guangdong colleges and universities (No.2021ZDZX2043), Natural Science Foundation of Guangdong Province (No.2022A1515012045, No.2023A1515012573).

Institutional Review Board Statement: The animal study protocol was approved by the Institutional Review Board of Experimental Animal Center of Guangdong Pharmaceutical University (SCXK20130002 and 2015-9-18).

Informed Consent Statement: Not Applicable.

Data Availability Statement: The data supporting the findings of this study are available from the corresponding author upon reasonable request. The protein-protein interaction (PPI) network is constructed using the STRING database (version 12.0; https://string-db.org).

Acknowledgments: This work was supported by the National Natural Science Foundation of China (No.22074024, 21005022), Key scientific research platforms and projects of Guangdong colleges and universities (No.2021ZDZX2043), Natural Science Foundation of Guangdong Province (No.2022A1515012045, No.2023A1515012573).

Conflicts of Interest: The authors declare that the research was conducted in the absence of any commercial or financial relationships that could be construed as a potential conflict of interest.

Appendix A

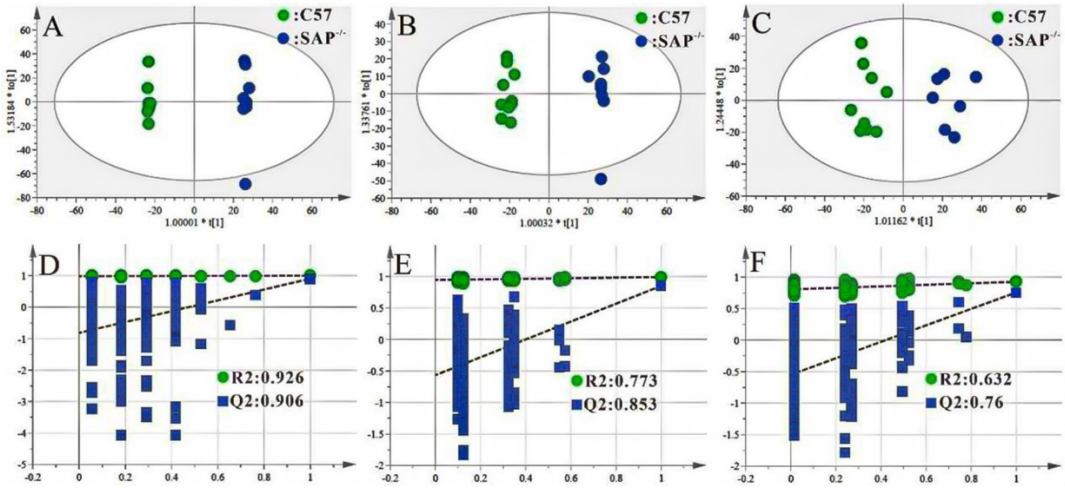

Figure A1. Metabolic differences between C57 and $SAP^{-/-}$ groups at three periods. OPLS-DA scores plots (**A**) (8 w), (**B**) (8 + 4 w), (**C**) (8 + 8 w) and the two hundred permutation checks (**D**) (8 w), (**E**) (8 + 4 w), (**F**) (8 + 8 w).

References

1. Loveless; R.W.; Floyd-O'Sullivan; Raynes; J.G.; Yuen; Feizi, T. Human serum amyloid P is a multispecific adhesive protein whose ligands include 6-phosphorylated mannose and the 3-sulphated saccharides galactose, N-acetylgalactosamine and glucuronic acid. *EMBO J.* **1992**, *11*, 813–819.
2. Jenny; N.S.; Arnold; A.M.; Kuller; L.H.; Tracy; R.P.; Psaty, B.M. Serum amyloid P and cardiovascular disease in older men and women: Results from the Cardiovascular Health Study. *Arterioscler. Thromb. Vasc. Biol.* **2007**, *27*, 352–358.
3. D.; Luo; T.; Xiong; H.; Liu; J.; Lu; H.; Li; M.; Hou; Y.; Guo; SAP, Z.; function, and its roles in immune-related diseases. *Int. J. Cardiol.* **2015**, *187*, 20–26.
4. Song; Z.; Cai; L.; Guo; L.; Tsukamoto; Y.; Yutani; C.; Li, X. Accumulation and expression of serum amyloid P component in human atherosclerotic lesions. *Atherosclerosis* **2010**, *211*, 90–95.
5. Cox; N.; Pilling; D.; Gomer, R.H. Serum amyloid P: A systemic regulator of the innate immune response. *J. Leukoc. Biol.* **2014**, *96*, 739–743.
6. Hutchinson, W.L.; Hohenester, E.; Pepys, M.B. Human serum amyloid P component is a single uncomplexed pentamer in whole serum. *Mol. Med.* **2000**, *6*, 482–493.
7. Pilely, K.; Fumagalli, S.; Rosbjerg, A.; Genster, N.; Skjoedt, M.; Perego, C.; Ferrante, A.M.R.; Simoni, M.D.; Garred, P. C-reactive protein binds to cholesterol crystals and co-localizes with the terminal complement complex in human atherosclerotic plaques. *Front. Immunol.* **2017**, *8*, 1040.
8. Gisterå, A.; Hansson, G.K. The immunology of atherosclerosis. *Nat. Rev. Nephrol.* **2017**, *13*, 368–380.
9. Richards, D.B.; Cookson, L.M.; Berges, A.C.; Barton, S.V.; Lane, T.; Ritter, J.M.; Fontana, M.; Moon, J.C.; Pinzani, M.;

Gillmore, J.D.; et al. Therapeutic clearance of amyloid by antibodies to serum amyloid P component. *N. Engl. J. Med.* **2015**, *373*, 1106–1114.
10. Desai, H.V.; Aronow, W.S.; Peterson, S.J.; Frishman, W.H. Cardiac amyloidosis: Approaches to diagnosis and management. *Cardiol. Rev.* **2010**, *18*, 1–11.
11. Pepys, M.B. Pathogenesis, diagnosis and treatment of systemic amyloidosis. *Philos. Trans. R. Soc. London Ser. B Biol. Sci.* **2001**, *356*, 203–211.
12. Li, X.A.; Hatanaka, K.; Ishibashi-Ueda, H.; Yutani, C.; Yamamoto, A. Characterization of serum amyloid P component from human aortic atherosclerotic lesions. *Arterioscler. Thromb. Vasc. Biol.* **1995**, *15*, 252–257.
13. Zheng, L.; Wu, T.; Zeng, C.; Li, X.; Li, X.; Wen, D.; Ji, T.; Lan, T.; Xing, L.; Li, J.; et al. SAP deficiency mitigated atherosclerotic lesions in ApoE$^{-/-}$ mice. *Atherosclerosis* **2016**, *244*, 179–187.
14. Li, Q.; Chen, W.; Huang, W.; Hou, R.; Huang, X.; Xu, M.; Que, L.; Wang, L.; Yang, Y. ^{1}H-NMR-Based Metabonomics Study to Reveal the Progressive Metabolism Regulation of SAP Deficiency on ApoE$^{-/-}$ Mice. *Metabolites* **2022**, *12*, 1278.
15. Iida, M.; Harada, S.; Takebayashi, T. Application of metabolomics to epidemiological studies of atherosclerosis and cardiovascular disease. *J. Atheroscler. Thromb.* **2019**, *26*, 747–757.
16. Crook, A.A.; Powers, R. Quantitative NMR-based biomedical metabolomics: Current status and applications. *Molecules* **2020**, *25*, 5128.
17. Tzoulaki, I.; Castagné, R.; Boulangé, C.L.; Karaman, I.; Chekmeneva, E.; Evangelou, E.; Ebbels, T.M.D.; Kaluarachchi, M.R.; Chadeau-Hyam, M.; Mosen, D.; et al. Serum metabolic signatures of coronary and carotid atherosclerosis and subsequent cardiovascular disease. *Eur. Heart J.* **2019**, *40*, 2883–2896.
18. Li, B.; Lu, X.; Wang, J.; He, X.; Gu, Q.; Wang, L.; Yang, Y. The metabonomics study of P-selectin glycoprotein ligand-1 (PSGL-1) deficiency inhibiting the progression of atherosclerosis in LDLR$^{-/-}$ mice. *Int. J. Biol. Sci.* **2018**, *14*, 36–46.
19. Chen, W.; Li, Q.; Hou, R.; Liang, H.; Zhang, Y.; Yang, Y. An integrated metabonomics study to reveal the inhibitory effect and metabolism regulation of taurine on breast cancer. *J. Pharm. Biomed. Anal.* **2022**, *214*, 114711.
20. Mora-Ortiz, M.; Ramos, P.N.; Oregioni, A.; Claus, S.P. NMR metabolomics identifies over 60 biomarkers associated with Type II Diabetes impairment in db/db mice Metabolomics. *Off. J. Metabolomic Soc.* **2019**, *15*, 89.
21. Meng, Z.; Tian, S.; Yan, J.; Jia, M.; Yan, S.; Li, R.; Zhang, R.; Zhu, W.; Zhou, Z. Effects of perinatal exposure to BPA, BPF and BPAF on liver function in male mouse offspring involving in oxidative damage and metabolic disorder. *Environ. Pollut.* **2019**, *247*, 935–943.
22. Jin, M.; Pan, T.; Tocher, D.R.; Betancor, M.B.; Monroig, Ó.; Shen, Y.; Zhu, T.; Sun, P.; Jia, L.; Zhou, Q. Dietary choline supplementation attenuated high-fat diet-induced inflammation through regulation of lipid metabolism and suppression of NFκB activation in juvenile black seabream (*Acanthopagrus schlegelii*). *J. Nutr. Sci.* **2019**, *8*, e38.
23. Rajabi, A.A.; Castro, G.S.F.; Silva, R.P.D.; Nelson, R.C.; Thiesen, A.; Vannucchi, H.; Vine, D.F.; Proctor, S.D.; Field, C.J.; Curtis, J.M.; et al. Choline supplementation protects against liver damage by normalizing cholesterol metabolism in Pemt/Ldlr knockout mice fed a high-fat diet. *J. Nutr.* **2014**, *144*, 252–257.
24. Poulsen, E.T.; Pedersen, K.W.; Marzeda, A.M.; Enghild, J.J. Serum amyloid P component (SAP) interactome in human plasma containing physiological calcium levels. *Biochemistry* **2017**, *56*, 896–902.
25. Fernstrom, J.D.; Fernstrom, M.H. Tyrosine, phenylalanine, and catecholamine synthesis and function in the brain2. *J. Nutr.* **2007**, *137*, 1539S–1547S.
26. Murín, R.; Mohammadi, G.; Leibfritz, D.; Hamprecht, B. Glial metabolism of valine. *Neurochem. Res.* **2009**, *34*, 1195–1203.
27. Mahdy, A.M.; Webster, N.R. Histamine and antihistamines. *Anaesth. Intensive Care Med.* **2011**, *12*, 324–329.
28. Rao, K.V.R.; Reddy, P.V.B.; Tong, X.; Norenberg, M.D. Brain edema in acute liver failure: Inhibition by L-histidine. *Am. J. Pathol.* **2010**, *176*, 1400–1408.
29. Falany, C.N.; Johnson, M.R.; Barnes, S.; Diasio, R.B. Glycine and taurine conjugation of bile acids by a single enzyme. Molecular cloning and expression of human liver bile acid CoA: Amino acid N-acyltransferase. *J. Biol. Chem.* **1994**, *269*, 19375–19379.
30. Schaffer, S.W.; Jong, C.J.; Ramila, K.C.; Azuma, J. Physiological roles of taurine in heart and muscle. *J. Biomed. Sci.* **2010**, *17*, S2.
31. Ansari, F.A.; Ali, S.N.; Mahmood, R. Taurine mitigates nitrite-induced methemoglobin formation and oxidative damage in human erythrocytes. *Environ. Sci. Pollut. Res. Int.* **2017**, *24*, 19086–19097.
32. Ding, L.; Chang, M.; Guo, Y.; Zhang, L.; Xue, C.; Yanagita, T.; Zhang, T.; Wang, Y. Trimethylamine-N-oxide (TMAO)-induced atherosclerosis is associated with bile acid metabolism. *Lipids Health Dis.* **2018**, *17*, 286.